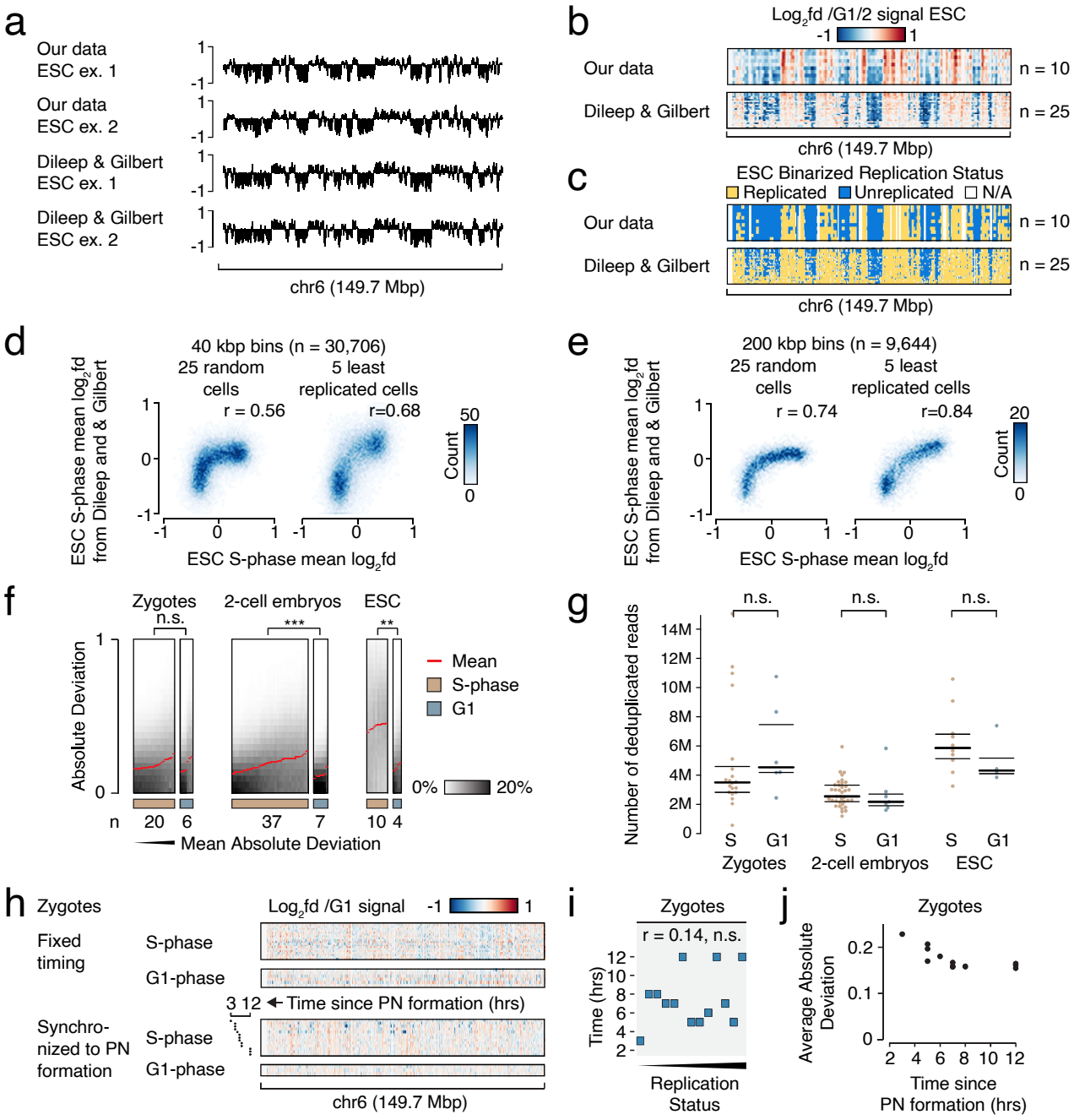

Supplementary Figure 1: Single embryo Repli-seq reveals atypical replication timing profiles in the early embryo.

a) Normalized log-2 fold Repli-seq read densities in two ESCs compared to similar profiles from two published mouse ESCs at chromosome 6.

b) Heatmaps of normalized log2-fold Repli-seq read densities in ESCs (n=10) compared to profiles from published ESCs (n=25) at chromosome 6.

c) Heatmaps showing individual binarized replication status of S-phase ESCs (n=10) compared to profiles from published mouse ESCs (n=25) at chromosome 6.

d, e) Scatter plots between mean normalized ESCs to published mouse ESCs quantified in 40kbp windows (d) or 200 kbp windows (e). Left side plots are from 25 random published cells and rightmost plot are from five cells with the lowest binarized Replication Score (R-values, Spearman's correlation coefficients).

f) Heatmaps of absolute genome-wide deviation in individual Repli-seq S- and G1- phase samples ranked according to the mean absolute deviation (red curves) (P-values, two-sided Mann-Whitney U-tests Benjamini-Hochberg corrected for multiple testing). ***: adjusted p-value < 0.001; **: adjusted p-value < 0.01; n.s.: not significant.

g) Beeswarm plots of the number of deduplicated mapped reads in each Repli-seq sample. Black bars indicate the 25, 50, and 75 percentiles (P-values, two-sided Welch Two-sample t-tests showing no significance (no correction for multiple testing)).

h) Heatmaps showing individual normalized Repli-seq read densities in S- and G1-phase zygotes (n=20) compared to similar profiles from S- and G1-phase zygotes where the fertilization time is reduced to one hour and the timing from pronucleus formation is recorded (n=13) at chromosome 6. Values are log2-fold differences relative to the G1-phase signal for each batch. Incubation time from pronucleus formation is illustrated in the small left side plot.

i) Tile plot showing relationships between Incubation time from pronucleus formation and ranked Replication Score from Repli-seq data in mouse zygotes. r- and p-values were obtained using Spearman's rank correlation tests.

j) Scatter plot showing the relationship between incubation time from pronucleus formation (X-axis) and mean absolute genome-wide deviation in log2 fold differences between Repli-seq of S-phase Zygotes and mean G1-phase Zygotes (Y-axis).

Source data are provided as a Source Data file.

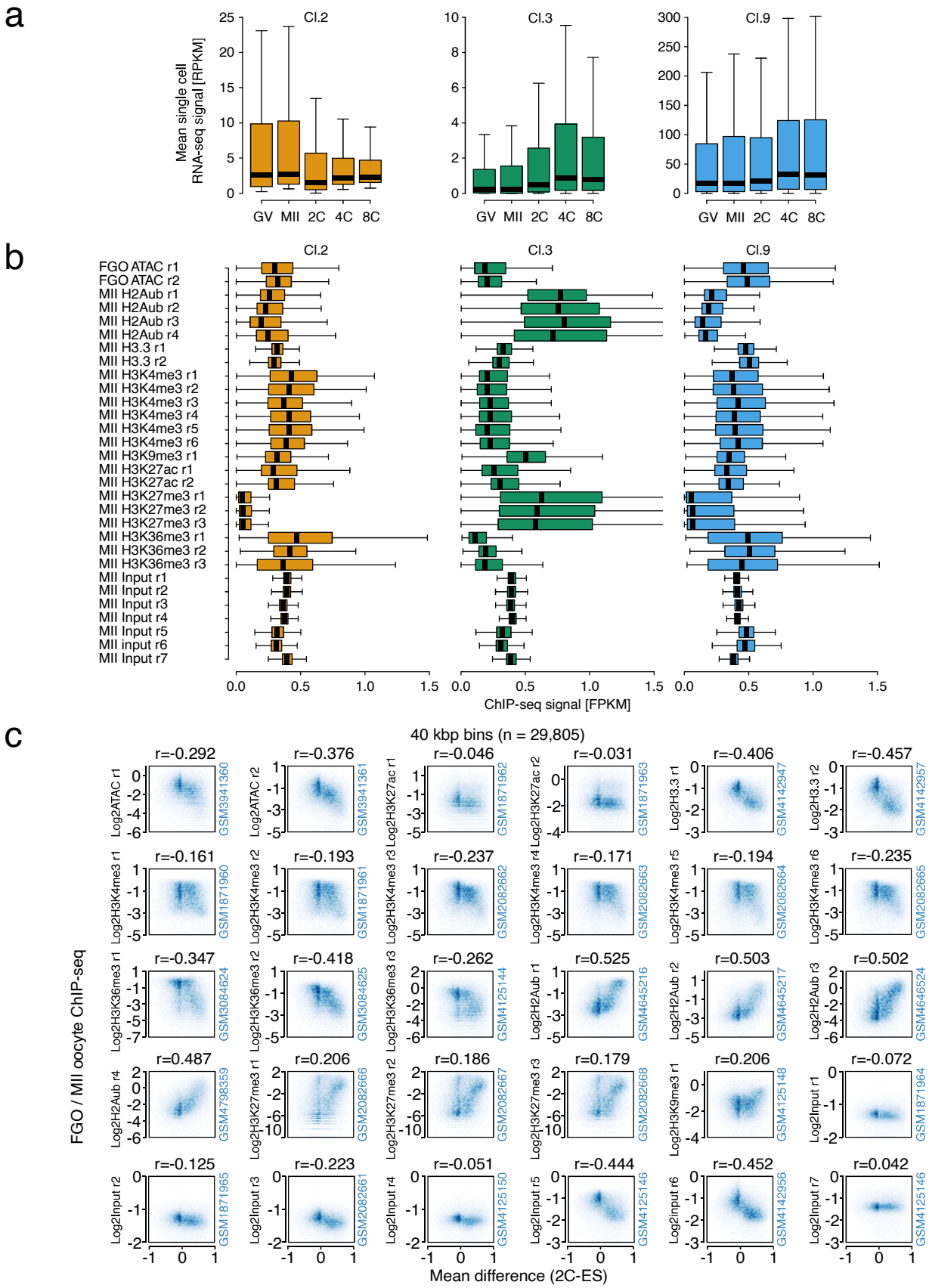

Supplementary Figure 2: Analysis of mean replication status difference between 2-cell embryos and ESCs in comparison to oocyte and embryo RNA-seq, Chip-seq and chromatin accessibility data.

a) Boxplots showing the transcript density in single oocyte or embryo RNA-seq quantified in 40kbp bins within three selected clusters (clusters 2, 3, and 9) from Figure 2c. Horizontal bands show medians, bars the interquartile range, and whiskers data points within 1.5x the interquartile range of the lowest and highest quartiles. RPKM: Reads per kilobasepair per million.

b) Boxplots showing the density of histone marks, histone variants, and chromatin accessibility in mouse oocytes quantified in 40kbp bins within three selected clusters (clusters 2, 3, and 9) from Figure 2b. Horizontal bands show medians, bars the interquartile range, and whiskers data points within 1.5x the interquartile range of the lowest and highest quartiles. FPKM: Fragments per kilobasepair per million.

c) Scatter plots showing the genome-wide relationship of the mean binarized replication status difference between 2-cell embryos and ESCs (X-axis) compared to oocyte histone marks, histone variants, and chromatin accessibility (Y-axis). Values were quantified in 40kbp windows and r-values indicate Pearson correlation coefficients. Blue vertical numbers are GEO accession numbers for individual datasets.

Source data are provided as a Source Data file.

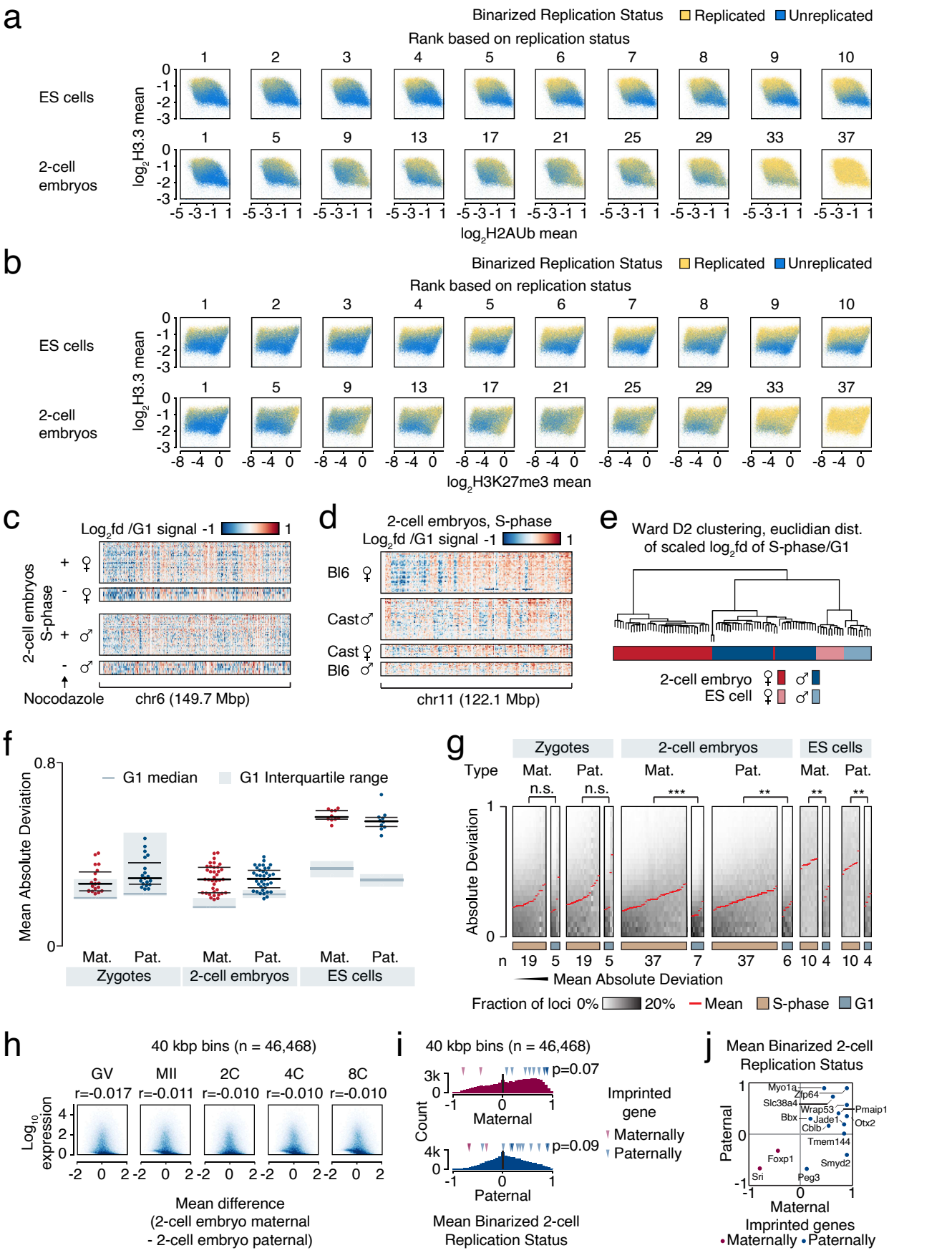

Supplementary Figure 3: Analysis of Polycomb Repressive Complex-mediated histones, imprinted genes and S/G1 deviation.

a, b) Heatmaps showing genome-wide relationships between mean binarized replication status in ESCs (top) and 2-cell embryos (bottom) relative to (a) mean enrichment of the H2AUb histone marks and H3.3 histone variant, (b) relative to mean enrichment of the H3K27me3 histone mark and H3.3 histone variant in MII oocytes. Values were quantified in 40kbp windows. The replication status ranking is indicated in the header of each heatmap .

c) Heatmaps displaying normalized log-2 fold Repli-seq read densities in individual S- and G1-phase 2-cell embryos, treated with and without Nocodazole.

d) Heatmaps displaying normalized log-2 fold Repli-seq read densities in maternal and paternal genomes of individual S-phase 2-cell embryos, where female mice were from the Bl6 and males were from the CAST/EiJ strains, and vice versa.

e) Dendrogram of hierarchical clustering of Euclidian distances between Repli-seq enrichment profiles of maternal and paternal genomes in individual 2-cell and ESCs. Values were log2-fold differences and scaled to have equal mean and standard deviations prior to Wards D2 clustering.

Continued on next page

Supplementary Figure 3 (continued)

f) Beeswarm plots of mean absolute genome-wide deviation within the maternal and paternal genomes of S-phase 2-cell embryos. The background deviation of G1 controls (grey boxes) and the interquartile range and median (wide bars). Black bars indicate the 25, 50, and 75 percentiles.

g) Absolute genome-wide deviation within maternal and paternal genomes of S-phase 2-cell embryos in individual Repli-seq S- and G1- phase samples, ranked (red curves)(P-values, two-sided Mann-Whitney U-tests Benjamini-Hochberg corrected for multiple testing). ***: adjusted p-value < 0.001; **: adjusted p-value < 0.01; n.s.: not significant.

h) Genome-wide relationship between the mean binarized replication status in maternal and paternal genomes of S-phase 2-cell embryos (X-axis) compared to mean RNA-seq transcript density from single oocyte or embryo (Y-axis), r-values indicate Pearson correlation coefficients.

i) Genome-wide distribution of mean replication status (maternal, top and paternal, bottom) of 2-cell embryos. Triangles illustrate similar replication scores at the loci of 18 validated imprinted genes with allele-specific expression at day E3.5. P-value comparisons of the maternally and paternally imprinted genes (two-sided Mann-Whitney U-tests Benjamini-Hochberg corrected for multiple testing).

j) Maternal and paternal replication scores at 18 validated imprinted genes with allele-specific expression at day E3.5.

Source data are provided as a Source Data file.

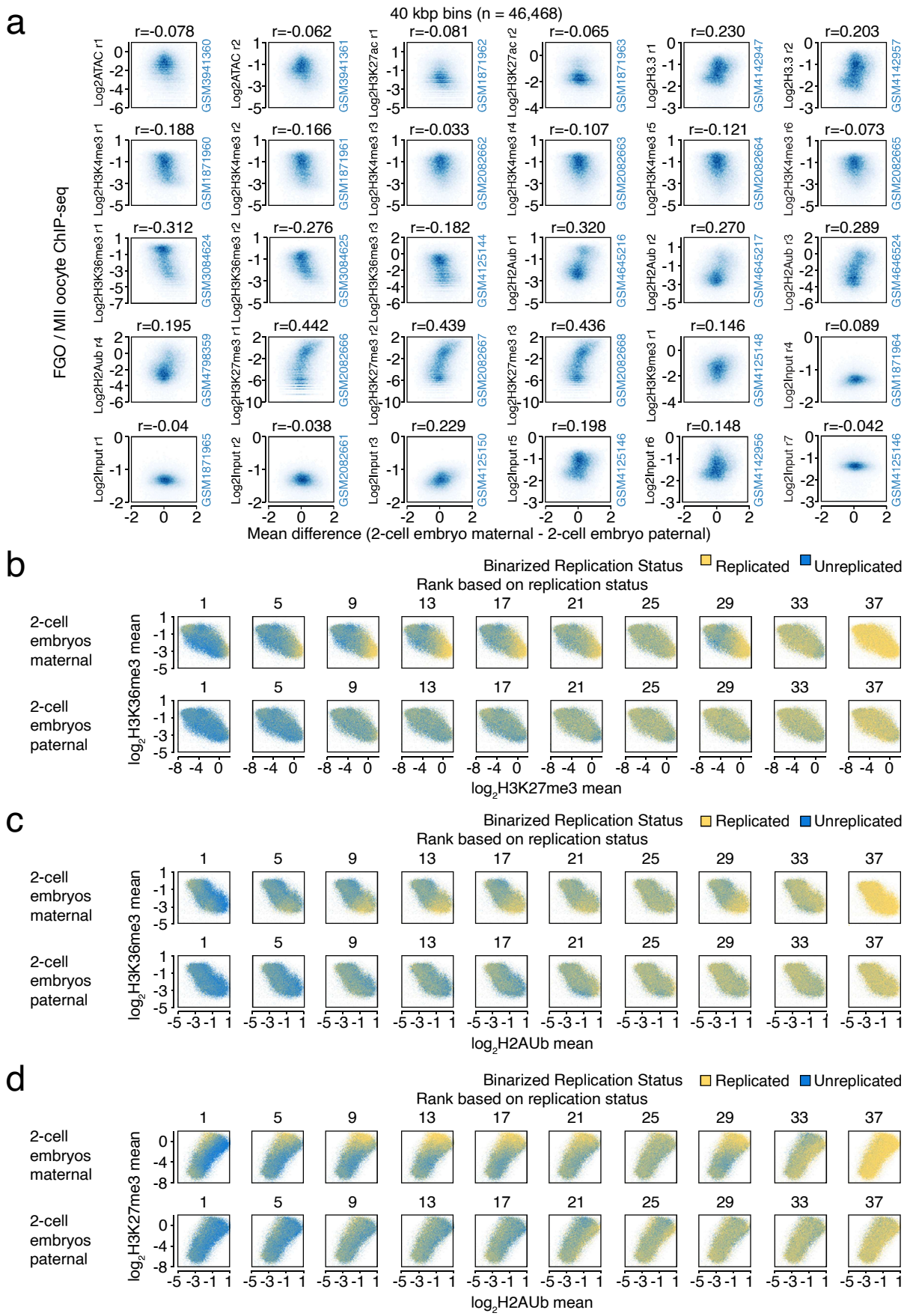

Supplementary Figure 4: Insights into parental genome-specific replication timing dynamics in 2-cell embryos through genome-wide MII oocyte ChIP-seq data.

a) Scatter plots showing the genome-wide relationship of the mean binarized replication status difference between maternal and paternal genomes of 2-cell mouse S-phase embryos (X-axis) compared to mouse oocyte histone marks, histone variants, and chromatin accessibility (Y-axis). Values were quantified in 40kbp windows and r-values indicate Pearson correlation coefficients. Blue vertical numbers are GEO accession numbers for individual datasets.

b-d) Heatmaps showing the genome-wide relationships between mean binarized replication status in individual maternal (top) and paternal (bottom) genomes of 2-cell mouse S-phase embryos and selected histone marks in mouse MII oocytes (X- and Y-axes). Axes represent: (b) mean enrichment of the H3K27me3 (X-axis) and H3K36me3 (Y-axis) histone marks, (c) mean enrichment of the H2AUb (X-axis) and H3K36me3 (Y-axis) histone marks, and (d) mean enrichment of the H2AUb (X-axis) and H3K27me3 (Y-axis) histone marks. Values were quantified in 40kbp windows. The horizontal order of each heatmap (and header) reflects the ranking based on the sum of the binarized values for each sample. Only every fifth sample is shown.

Source data are provided as a Source Data file.

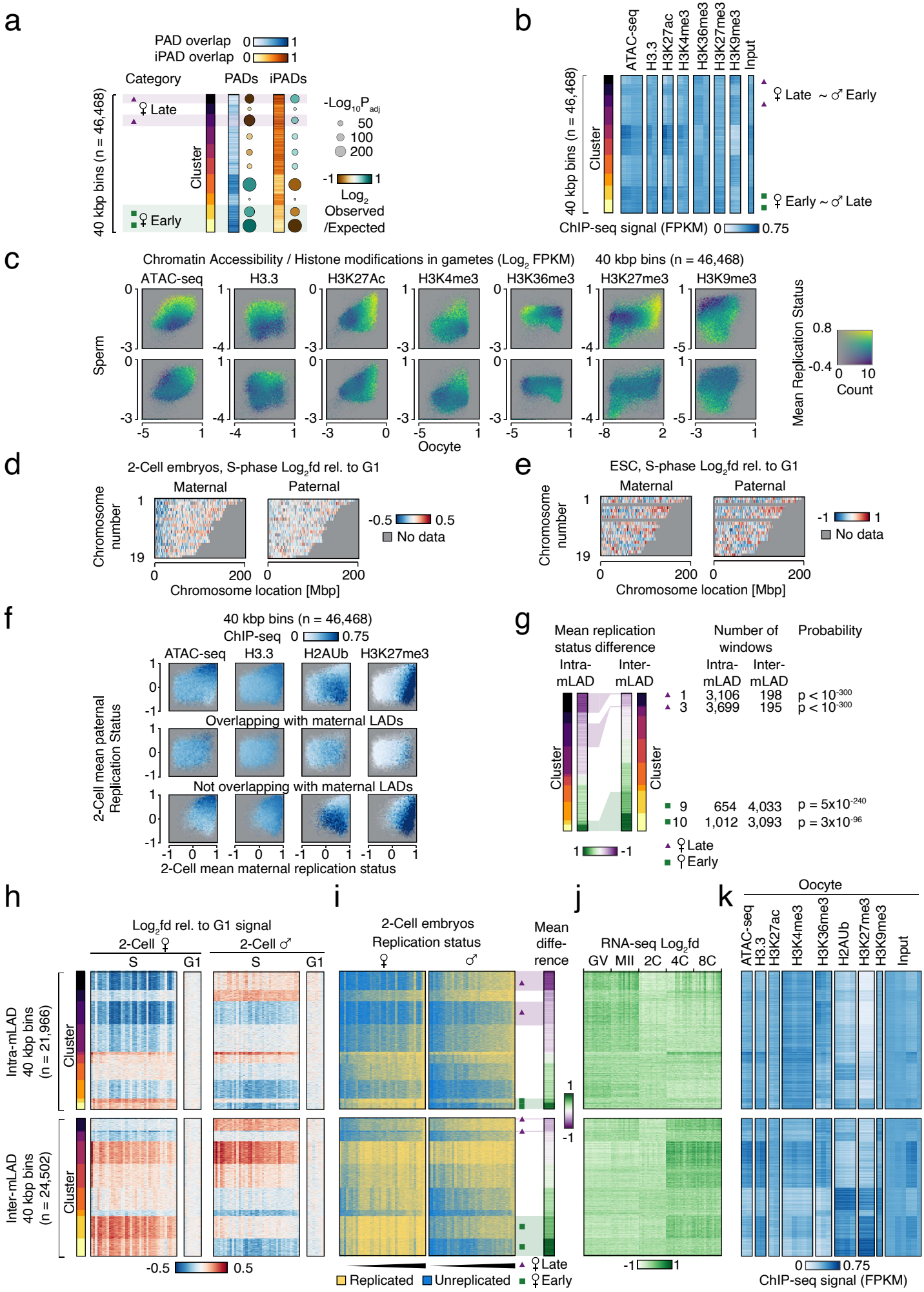

Supplementary Figure 5: Correlation of large scale 2-cell replication timing patterns with oocyte-specific histone marks, domains and higher-order structural domains.

a) Heatmaps with bubbles showing overlap with PADs and iiPADs, clustering as in Fig. 3c. Green squares and purple triangles indicate maternal early or late replication, respectively. p-values of overlap compared to expected numbers from randomly distributed overlaps from X^2 Benjamini-Hochberg tests corrected for multiple testing. Log2 fold values shows the observed overlap compared to expected.

Continued on next page

Supplementary Figure 5 (continued)

b) Genome-wide histone mark and chromatin accessibility signal from sperm cells. Bins ordered as in Fig. 3c, FPKM-normalized. Green squares and purple triangles, defined in Fig. 3d.

c) Heatmaps showing histone marks, histone variant, and chromatin accessibility in MII oocytes (X-axes), sperm cells (Y-axis), and mean binarized replication status in maternal (top) and paternal (bottom) genomes of 2-cell embryos.

d, e) Heatmaps of Repli-seq read densities in maternal (left) and paternal (right) genomes of 2-cell embryos (n=37) (d) and ESCs (n=10) (e). X-axis: chromosome coordinates, Y-axis: autosome number. Chromosomes 3 and 8 and were excluded from ESCs due to aneuploidy.

f) Heatmaps of oocyte histone marks, histone variant, and chromatin accessibility signal relative to mean maternal (X-axis) and paternal (Y-axis) binarized replication status. Values from the entire genome (top), within (middle), or outside (bottom) LADs in the maternal genome of 2-cell embryos.

g) Heatmaps of the mean binarized replication status difference between the 2-cell maternal and paternal genomes within (left) or outside (right) maternal 2-cell embryo LADs. Clustering as in Fig. 3c. Green squares and purple triangles indicate clusters with notably early or late replication, respectively. Numbers indicate 40kbp bins within each cluster inside or outside of LADs (P-values, X^2 tests Benjamini-Hochberg corrected for multiple testing).

h-k) Heatmaps showing the signal within or outside LADs in the maternal genome of 2-cell embryos. K-means clustering as in Figure 3c . (h) Genome-wide signal enrichment and variation in individual S- and G1-phase Repli-seq samples. (i) Genome-wide binarized replication status in individual 2-cell Repli-seq samples and Mean binarized replication status between the parental genomes. Green squares and purple triangles are clusters constituting regions with notably early or late maternal replication, respectively. (j) Transcript density difference from single oocyte or embryo RNA-seq and (k) genome-wide histone mark, histone variant and chromatin accessibility signal, FPKM-normalized.

Source data are provided as a Source Data file.